hexagon:2610.00676v1

EXISTENCE OF SRB MEASURES FOR SOME RÖSSLER SYSTEMS

THEOPHILE CABY

Laboratoire d'Océanographie Physique et Spatiale, Univ Brest, CNRS, Ifremer, IRD, Brest, France
theophile.caby@univ-brest.fr

Abstract. We prove that for the Rössler system $\dot{x} = -(y+z)$, $\dot{y} = x + ay$, $\dot{z} = b + z(x-c)$ with $a = b = 0.2$, the set of parameters c within $6 \cdot 10^{-5}$ of the classical value $c = 5.7$ for which the flow has a Hénon-like strange attractor supporting a Sinai–Ruelle–Bowen (SRB) measure has positive Lebesgue measure. The key step, proved with computer assistance, is that at an explicit parameter within $5.5 \cdot 10^{-5}$ of 5.7 the period-one saddle of the Poincaré map has a quadratic homoclinic tangency that unfolds generically; the conclusion then follows from the theorems of Mora–Viana, Benedicks–Young and Benedicks–Viana. The same method gives two further such tangencies near 5.7 and one at the band-merging parameter $c \approx 4.507$. The proof reduces the generic-tangency conditions to finitely many inequalities, through explicit C^2 graph-transform bounds for the local invariant manifolds of a Poincaré map whose area contraction is of order 10^{-11}–10^{-14}, and a scalar tangency function. The inequalities are checked with interval arithmetic in CAPD and re-checked with an independent implementation based on the Kv library; the analytic tangency criterion is formalised in Lean 4. Whether an SRB measure exists at $c = 5.7$ itself remains open.

1. Introduction

The Rössler system [30]

$$\dot{x} = -(y+z), \qquad \dot{y} = x + ay, \qquad \dot{z} = b + z(x-c) \tag{1}$$

is one of the simplest three-dimensional flows with an apparently chaotic attractor. At the classical parameters $(a, b, c) = (0.2, 0.2, 5.7)$, numerical simulations show a strange attractor whose first return map to a transversal section is, to all visible precision, a unimodal interval map. A natural mathematical question is whether this attractor carries a *Sinai–Ruelle–Bowen (SRB) measure*: an invariant probability with a positive Lyapunov exponent whose conditional measures along unstable manifolds are absolutely continuous. Such a measure describes the statistics of a set of initial conditions of positive volume (see [38] for a survey).

For uniformly hyperbolic and singular-hyperbolic attractors, SRB measures are well understood. In particular, Tucker's computer-assisted proof [32] showed that the Lorenz equations have a singular-hyperbolic attractor, and such attractors support an SRB measure [1]. The decisive feature there is that singular hyperbolicity is an *open* condition, defined by invariant cone fields, which can be certified by a finite computation.

The Rössler attractor is of a different nature. Its return map folds, so no invariant cone field can exist near the fold; the attractor is at best non-uniformly hyperbolic, of Hénon type. For such systems, horseshoes of positive entropy are robust, but the existence of SRB measures is a delicate, parameter-dependent property. For the Hénon family it has been proved only for

Date: October 30, 2026.

2020 *Mathematics Subject Classification.* 37D25, 37D45, 37C40, 37M21, 65G40, 68V15.

Key words and phrases. Rössler system, homoclinic tangency, strange attractors, SRB measures, computer-assisted proof, interval arithmetic, Lean.

positive-measure, Cantor-like sets of parameters [5, 7, 25, 6], and the question remains open at the classical Hénon parameters.

Moreover, spiral attractors of Rössler type are *quasi-attractors* in the sense of Afraimovich–Shilnikov: stable periodic orbits of long period are present, or appear under arbitrarily small perturbations [16]. Galias [14] recently fixed $c = 5.7$, varied $a = b$ jointly, and proved with interval arithmetic that the system has a stable periodic orbit (of period 97 for the return map) for parameters in a periodic window of width about $4 \cdot 10^{-38}$ at distance less than $2 \cdot 10^{-22}$ from the classical value $a = b = 0.2$. His results indicate that periodic windows are dense near the classical parameters, and the widths of the windows he found provide, in his words, a strong argument that the classical attractor itself is not periodic. In any case, "having an SRB measure" is not an open condition in parameter space, and it cannot be certified at a given parameter value by verifying an open condition, as was done for the Lorenz attractor.

Rigorous results on the Rössler system so far concern topological dynamics and periodic orbits:

- symbolic dynamics and positive topological entropy at the classical parameters [39];
- a trapping region for the return map [20];
- period doubling [36];
- periodic orbits of all periods at $c = 5.25$, and of all periods except 3 at $c = 4.7$ [15];
- for $b = 0.2$, $c = 15$ and $a \in [0.12, 0.3659]$, a trapping region of the Poincaré map containing a connected attractor of positive topological entropy, whose entropy grows through a sequence of bifurcations of periodic orbits [34];
- periodic windows extremely close to the classical parameters [14];
- a reduction of the non-wandering set to the quadratic family [18].

The "chaos" established in [39, 34] is topological: these works prove the existence of invariant sets carrying symbolic dynamics, hence positive topological entropy. Such sets are typically of Lebesgue measure zero and may coexist with a periodic sink, so they do not decide whether the attractor observed in simulations is chaotic in the metric sense (positive Lyapunov exponent for typical orbits, or an SRB measure); that question is open at the classical parameters, see [14]. To our knowledge, no SRB measure had been established for any parameter of the Rössler family.

Main result. Fix $a = b = 0.2$, and let P_c denote the Poincaré map of (1) on the section $\Sigma = \{x = 0,\ \dot{x} > 0\}$, written in the coordinates (y, z).

Main Theorem. *There is a parameter c_* with $|c_* - 5.7| < 5.47 \cdot 10^{-5}$ such that, for every $\varepsilon > 0$, the set of $c \in (c_* - \varepsilon, c_* + \varepsilon)$ for which the Rössler flow (1) with $a = b = 0.2$ has a Hénon-like strange attractor supporting an ergodic SRB measure, whose basin has positive Lebesgue measure in $\mathbb{R}^3$, has positive Lebesgue measure. In particular, the set of such parameters c in $(5.7 - 6 \cdot 10^{-5},\ 5.7 + 6 \cdot 10^{-5})$ has positive Lebesgue measure.*

The parameter c_* is explicit: it lies in the interval $J_3 \subset (5.70005464309,\ 5.70005464312)$ of (4). The proof has two parts of different nature.

- *The new ingredient*, proved with computer assistance (Proposition 5.1): at $c = c_*$ the period-one saddle p_c of P_c has a quadratic homoclinic tangency that unfolds generically as c varies. In the (almost one-dimensional) return map, this corresponds to the critical point landing on p after 16 iterates (Figure 1).
- *The passage from such a tangency to SRB measures* (Proposition 3.5), which relies on the theorem of Mora and Viana [25] on the abundance of strange attractors in generic unfoldings of homoclinic tangencies, on the construction of SRB measures for these attractors and

the solution of the basin problem [7, 6, 33], and on a standard suspension argument. One hypothesis of [25], the smooth linearisability of the saddle, is not verified here; for it we rely on later work in which it was removed [29, 17] (Remark 3.2).

The same argument gives positive-measure sets of SRB parameters accumulating at two further tangency parameters, at distances less than $5.81\cdot10^{-4}$ and $4.21\cdot10^{-4}$ from 5.7 (Proposition 5.1), and at the parameter $c \approx 4.507$ where the two bands of the chaotic attractor of the period-doubling cascade merge (Proposition 6.1).

These results say nothing about the classical value $c = 5.7$ itself. Nor do they identify the attractors they produce with the large attractor seen in simulations: they are the small Hénon-like attractors created near the orbit of tangency. We return to these points in Section 8.

Method. A quadratic, generically unfolding tangency is characterised by four conditions on a scalar function $g(s, c)$, which measures the signed distance from a parametrised piece of the unstable manifold to the local stable manifold:

$$g = 0, \qquad \partial_s g = 0, \qquad \partial_s^2 g \neq 0, \qquad \partial_c g \neq 0.$$

To make these conditions checkable, we need the local invariant manifolds of p_c with *second-order* control, including their dependence on c. We obtain this from explicit C^2 graph-transform estimates (Lemmas 4.2 and 4.3), which reduce everything to interval inequalities on the first and second derivatives of P_c over small boxes. The remaining quantities are derivatives of P_c^N along the unstable manifold, which we enclose with the C^2-Lohner algorithm of the CAPD library [20, 37]. Each verification takes a few seconds on one core.

The approach is close in spirit to the computer-assisted proof of a homoclinic tangency for the Hénon map and the forced damped pendulum by Wilczak and Zgliczyński [35], which uses covering relations and cone conditions in the projectivised tangent bundle; see also [2]. Coomes, Koçak and Palmer [12] recently gave a computable criterion for generic quadratic tangencies of a fixed point of a planar diffeomorphism depending on two parameters. It is based on Kleinkauf's characterisation of quadratic, generically unfolding tangencies through bounded solutions of the variational equations along the homoclinic orbit, and reduces the proof to the invertibility of a finite matrix built from a pseudo-orbit, via the implicit function theorem; it is illustrated on explicit planar maps (Hénon, Duffing, Bogdanov, Perennial Grass). Our setting and method are different. The map is a Poincaré map of a three-dimensional flow, known only through validated integration, and it is extremely dissipative: $|\lambda_s| \approx 10^{-11}$–$10^{-14}$, so the stable manifold is very well determined but the unstable fold is correspondingly thin. What our method provides is:

- explicit C^2 bounds on both local manifolds, together with their parameter dependence, from graph transforms whose contraction factors are about $2 \cdot 10^{-4}$ for W^u and 0.42 for W^s; the extreme dissipation is an advantage here rather than a difficulty;
- correlated (affine) enclosures of P_c^N for N up to 26;
- the generic-unfolding condition $\partial_c g \neq 0$ in a one-parameter family;
- the passage, via Mora–Viana, to SRB measures for the flow.

Independent checks. To reduce the trust placed in a single code base, we did two further checks.

- *Second implementation.* The hypotheses for J_1, J_3 and J_0, including the numerical statements of Propositions 5.1 and 6.1, were re-verified with a separately written program built on a different validated-numerics library, Kv [21] (Section 7.1). It computes the Poincaré map in a different way: as a fixed-angle map after reparametrising the flow by the polar angle.

- *Formal proof.* The analytic tangency criterion (Lemma 4.5) and the Taylor bound (Remark 4.6) were formalised and machine-checked in Lean 4 with Mathlib [26, 24] (Section 7.2).

Organisation. Section 2 fixes definitions. Section 3 shows that a generically unfolding tangency gives SRB measures (Proposition 3.5), listing the hypotheses of the theorems used. Section 4 reduces the existence of such a tangency to finitely many inequalities, which are verified in Section 5 near $c = 5.7$, where the Main Theorem is proved, and in Section 6 at the band-merging parameter. Section 7 describes the independent implementation, the Lean formalisation and the code audit. Section 8 discusses the classical parameter.

2. Setting and definitions

2.1. **The Poincaré map.** Let X_c denote the vector field (1) with $a = b = 0.2$, and let φ_c^t be its flow. The plane $\{x = 0\}$ is crossed transversally in the positive direction exactly on $\Sigma = \{(0, y, z) : \ y + z < 0\}$. For $q \in \Sigma$ whose forward orbit returns to Σ, let $\tau_c(q) > 0$ be the first return time and $P_c(q) = \varphi_c^{\tau_c(q)}(q)$. On the open set where it is defined, P_c is an injective local diffeomorphism, real analytic jointly in (q, c), because X_c is polynomial and the crossing is transversal. We use (y, z) as coordinates on Σ.

It is convenient to treat c as an additional state variable. The extended field $\hat{X}(x, y, z, c) = (X_c(x, y, z), 0)$ has a Poincaré map $\hat{P}(y, z, c) = (P_c(y, z), c)$ on $\{x = 0\}$, whose first and second derivatives contain all the c-derivatives we need. These are derivatives of the Poincaré map itself, including the correction for the varying return time: with $e_1 = (1, 0, 0)$,

$$DP_c(q) = \Big(I - \frac{X_c(P_c(q))\, e_1^T}{\dot{x}(P_c(q))}\Big) D\varphi_c^{\tau_c(q)}(q) \quad \text{restricted to } T_q\Sigma,$$

and similarly at second order and in the c-direction; Section 7.3 explains how they are computed.

2.2. **Orientation.** Since Σ is crossed in one direction only, P_c preserves orientation. Explicitly, for q in its domain,

$$\det DP_c(q) = \exp\Big(\int_0^{\tau_c(q)} \operatorname{div} X_c(\varphi_c^t q)\, dt\Big)\, \frac{\dot{x}(q)}{\dot{x}(P_c(q))} > 0,$$

because $\dot{x} = -(y + z) > 0$ on Σ. (Compare the volumes spanned by X_c, e_y, e_z at q and their images under $D\varphi_c^{\tau_c(q)}$, and use Liouville's formula.) At a fixed point the last factor equals 1. In particular, if p is a saddle fixed point with $\lambda_u < -1$, then $\lambda_s = \det DP_c(p)/\lambda_u < 0$.

2.3. **Homoclinic tangencies.** Let $(F_c)_{c \in I}$ be a C^2 family of injective local diffeomorphisms of an open subset of $\mathbb{R}^2$, and let p_c be a hyperbolic saddle fixed point of F_c depending C^2 on c.

Definition 2.1. We say that F_{c_*} has a *quadratic homoclinic tangency associated to p_{c_*}, unfolding generically at c_**, if there exist

- an open set $\mathcal{U} \subset \mathbb{R}^2$ and an interval $I' \ni c_*$;
- a C^2 function $\ell \colon \mathcal{U} \times I' \to \mathbb{R}$ with $\nabla_q \ell \neq 0$, such that for each c the zero set $\{\ell(\cdot, c) = 0\}$ is an arc of $W^s(p_c)$;
- a C^2 map $\Gamma \colon (s_0 - \eta, s_0 + \eta) \times I' \to \mathcal{U}$ with $\partial_s \Gamma \neq 0$ and $\Gamma(s, c) \in W^u(p_c)$;

such that the function $g(s, c) = \ell(\Gamma(s, c), c)$ satisfies

$$g(s_0, c_*) = 0, \qquad \partial_s g(s_0, c_*) = 0, \qquad \partial_s^2 g(s_0, c_*) \neq 0, \qquad \partial_c g(s_0, c_*) \neq 0.$$

Remark 2.2. The conditions are independent of the choice of the defining function ℓ and of the regular parametrisation Γ. Straightening $W^s(p_c)$ to $\{x_2 = 0\}$, the unstable arc becomes, near the tangency point, a graph $x_2 = \alpha x_1^2 + \beta(c - c_*) + \dots$, with $\alpha \neq 0$ equivalent to $\partial_s^2 g \neq 0$ and $\beta \neq 0$ to $\partial_c g \neq 0$. These are the two conditions of a generic unfolding of a homoclinic tangency in the sense of Palis–Takens [28] and of Mora–Viana [25, p. 6]: in the normal form of [25], $f_\mu^N(1 + \xi, \eta) = (\alpha\xi^2 + \beta\eta + v\mu + \dots, 1 + \dots)$ with $\alpha \neq 0$ and $v \neq 0$. See also [35, Def. 4].

2.4. **SRB measures and strange attractors.** Let F be a C^2 diffeomorphism (or flow) and μ an ergodic invariant Borel probability measure with compact support. We call μ an *SRB measure* if it has a positive Lyapunov exponent μ-almost everywhere (for flows, one transverse to the flow direction), and its conditional measures on local unstable manifolds are absolutely continuous with respect to the induced Riemannian measure. The *basin* of μ is the set of points q whose empirical measures $\frac{1}{n}\sum_{k<n} \delta_{F^k q}$ (respectively $\frac{1}{T}\int_0^T \delta_{\varphi^t q}\, dt$) converge weakly* to μ.

Following [25, p. 2], an *attractor* of a surface map is a compact invariant set Λ with a dense orbit whose stable set $W^s(\Lambda)$ (its topological basin) has non-empty interior; it is *strange* if it contains a dense orbit with a positive Lyapunov exponent. We call *Hénon-like* the strange attractors produced by the renormalisation of [25] near a homoclinic tangency (Theorem 3.1); they are not uniformly hyperbolic [25, p. 2]. For the Rössler flow, a Hénon-like strange attractor is the flow saturation $\{\varphi_c^t q : q \in \Lambda,\ t \in \mathbb{R}\}$ of a Hénon-like strange attractor $\Lambda \subset \Sigma$ of P_c. By the flow-box theorem, its basin also has non-empty interior.

3. From homoclinic tangencies to SRB measures

We use three results on generic unfoldings of homoclinic tangencies of surface maps. We state them in the form in which we use them, with precise references.

Theorem 3.1 (Mora–Viana [25, Theorem A and §2])**.** *Let $(f_\mu)_\mu$ be a C^∞ one-parameter family of surface diffeomorphisms such that f_0 has a homoclinic tangency associated to a hyperbolic fixed point p_0, with the following properties ([25, pp. 5–6]):*

(MV1) *the saddle is dissipative: $|\det Df_\mu(p_\mu)| < 1$;*
(MV2) *its eigenvalues satisfy $0 < \lambda < 1 < \sigma$;*
(MV3) *there are μ-dependent C^r linearising coordinates for f_μ in a neighbourhood of p_μ, for a fixed, sufficiently large r;*
(MV4) *the tangency is quadratic and unfolds generically with μ (Remark 2.2).*

Then, for parameter intervals I_n converging to $\mu = 0$ and neighbourhoods U_n of a point of the orbit of tangency, suitable rescalings of $f_\mu^{n+N}|U_n$, $\mu \in I_n$, converge in the C^r topology to the quadratic family $(a, x, y) \mapsto (1 - ax^2, 0)$ and form a Hénon-like family in the sense of [25, Theorem 2.1]*; and for n large there is a set $E_n \subset I_n$ of positive Lebesgue measure such that, for $\mu \in E_n$, the map $f_\mu^{n+N}|U_n$ has a strange attractor* [25, Theorem B]*. In particular, for every $\varepsilon > 0$ the set of $\mu \in (-\varepsilon, \varepsilon)$ for which f_μ has a strange attractor near the orbit of tangency has positive Lebesgue measure.*

Remark 3.2 (on the hypotheses). We comment on each hypothesis, for the family $f_\mu = P^2_{c_*+\mu}$ used in the proof of Proposition 3.5.

- *Regularity.* (P_c) is real analytic in (q, c).
- (MV1), (MV2): $\det DP_c^2(p_c) = (\lambda_u\lambda_s)^2 < 1$, and the eigenvalues of $DP_c^2(p_c)$ are $\lambda_s^2 \in (0, 1)$ and $\lambda_u^2 > 1$. (Mora and Viana work with positive eigenvalues, which can always be achieved by passing to the second iterate, as we do for our flip saddle.)
- (MV4) is exactly what Definition 2.1 encodes; P^2 has the same invariant manifolds, tangency and function g as P.

- (MV3) is *not* verified here. By Sternberg's theorem [31], C^r linearising coordinates exist, depending smoothly on the parameter, when the eigenvalues satisfy finitely many non-resonance conditions $\lambda^i\sigma^j \neq \lambda, \sigma$ $(2 \leq i+j \leq k(r))$; this is a generic condition, but our enclosures of λ_s do not allow us to check it at c_*. As noted by Barrientos and Rojas [3, footnote 4], smooth linearisation is not necessary: the linearisability conditions were removed in the renormalisation schemes of Romero [29] and of Gonchenko, Shilnikov and Turaev [17]. We rely on these works for this point.
- Barrientos and Rojas also report [3, footnote 2] that the proof of [25] needs an additional assumption on the distortion of the determinant of the family, and that this assumption seems unnecessary in view of Berger's alternative approach [8]. In the linearised setting of [25, §2], the bounds on the derivatives of $\det D\varphi_a$ required of a Hénon-like family are part of the conclusion of [25, Theorem 2.1]; we have not been able to determine whether this addresses the point raised in [3].

Theorem 3.3 (Benedicks–Young [7], Benedicks–Viana [6]; see [33, §4, Theorems 3 and 4])**.** *In the situation of Theorem 3.1, after replacing each E_n by a subset of positive Lebesgue measure, the strange attractor Λ of $f_\mu^{n+N}|U_n$, $\mu \in E_n$, given by Theorem 3.1 supports a unique SRB measure, and Lebesgue-almost every point of the topological basin of Λ belongs to the basin of this measure.*

Benedicks and Young [7] constructed SRB measures for the Hénon attractors of Benedicks and Carleson [5]. Benedicks and Viana [6] proved, for a large class of non-uniformly hyperbolic attractors of dissipative diffeomorphisms, that there are no "holes" in the basin: Lebesgue-almost every point of the topological basin is generic for the SRB measure. Their analysis is carried out in the setting of the Hénon-like families of Mora and Viana [4, §3], and Viana [33, §4] states both results for Hénon-like attractors, including those arising in generic unfoldings of homoclinic tangencies, under the strong area dissipativeness that holds for the renormalised maps of Theorem 3.1. Mora and Viana had anticipated this extension [25, p. 3].

Both theorems are local: all the maps and iterates they use are defined on a neighbourhood of the closure of the orbit of tangency, on which P_c is an analytic diffeomorphism onto its image, depending analytically on c. They therefore apply to the family (P_c).

Lemma 3.4 (suspension)**.** *Let $\Lambda \subset \Sigma$ be a compact P_c-invariant attractor in the domain of P_c, and let ν be an ergodic SRB measure of P_c supported on Λ whose basin meets the topological basin of Λ in a set of positive area. Then*

$$\mu = \frac{1}{\int \tau_c \, d\nu} \int_\Lambda \int_0^{\tau_c(q)} \delta_{\varphi_c^t q} \, dt \, d\nu(q)$$

is an ergodic SRB measure for the flow φ_c^t, supported on the flow saturation of Λ, and its basin has positive Lebesgue measure in $\mathbb{R}^3$.

Proof. This is standard; we indicate the main points. Let V be a compact neighbourhood of Λ in Σ on which τ_c is continuous and bounded away from 0 and ∞. Invariance and ergodicity are classical for suspension flows. The exponents of μ transverse to the flow are those of ν divided by $\int \tau_c \, d\nu$; in particular one is positive. The strong unstable manifold of φ_c through $q \in \Lambda$ projects diffeomorphically, along flow lines, onto $W^u(q; P_c)$, so absolute continuity of conditional measures is preserved. For the basin, let $q \in B(\nu)$ lie in the topological basin of Λ, so that $P_c^k q \in V$ for all large k. For continuous ψ, the flow averages of ψ along q are, up to an error bounded by $\sup|\psi| \sup_V \tau_c/T$, ratios of Birkhoff sums of the continuous functions $\Psi(q) = \int_0^{\tau_c(q)} \psi(\varphi_c^t q) \, dt$ and τ_c, which converge to $\int \Psi \, d\nu / \int \tau_c \, d\nu = \int \psi \, d\mu$. Hence the basin of

μ contains the flow saturation of this set, which has positive volume because $(q,t) \mapsto \varphi_c^t q$ is a local diffeomorphism from $\Sigma \times (0,t_0)$ to $\mathbb{R}^3$ for small $t_0 > 0$. □

Proposition 3.5. *Let c_* be a parameter at which P_{c_*} has a saddle fixed point p_{c_*} with $|\det DP_{c_*}(p_{c_*})| < 1$, whose stable and unstable manifolds have a quadratic homoclinic tangency unfolding generically at c_* (Definition 2.1). Then, for every $\varepsilon > 0$, the set of $c \in (c_* - \varepsilon, c_* + \varepsilon)$ for which the Rössler flow (1) with $a = b = 0.2$ has a Hénon-like strange attractor supporting an ergodic SRB measure, whose basin has positive Lebesgue measure in $\mathbb{R}^3$, has positive Lebesgue measure.*

Proof. By Section 2, $0 < \det DP_{c_*}(p_{c_*}) < 1$, so the two multipliers of the saddle have the same sign, and $f_\mu = P^2_{c_*+\mu}$ has positive multipliers $\lambda_s^2 \in (0,1)$ and $\lambda_u^2 > 1$. We apply Theorems 3.1 and 3.3 to (f_μ), whose hypotheses are discussed in Remark 3.2.

Fix $\varepsilon > 0$. We obtain a set $\mathcal{E} \subset (c_* - \varepsilon, c_* + \varepsilon)$ of positive measure such that, for $c \in \mathcal{E}$, an iterate $F = P_c^m$ (with $m = 2(n+N)$) restricted to a small open set U has a strange attractor Λ supporting an SRB measure ν_0 as in Theorem 3.3. Let $\Lambda' = \bigcup_{j<m} P_c^j(\Lambda)$. It is compact and P_c-invariant; the P_c-orbit of a point whose F-orbit is dense in Λ is dense in Λ', and its Lyapunov exponent for P_c is that for F divided by m, hence positive; and the stable set of Λ' contains that of Λ, which has non-empty interior. So Λ' is a strange attractor of P_c. The measure $\nu = \frac{1}{m}\sum_{j<m} (P_c^j)_* \nu_0$ is an ergodic SRB measure of P_c supported on Λ': push-forwards by diffeomorphisms preserve absolute continuity along unstable manifolds. Its basin contains the basin of ν_0 for F, which by Theorem 3.3 has full Lebesgue measure in the topological basin of Λ, a set with non-empty interior. Lemma 3.4 concludes the proof. □

4. Reduction to finitely many inequalities

4.1. **Interval notation and local coordinates.** For a compact interval $[x]$ we write $\mathrm{mag}[x] = \max\{|x| : x \in [x]\}$ and $\mathrm{mig}[x] = \min\{|x| : x \in [x]\}$. Arithmetic on intervals is the usual set-valued arithmetic with outward rounding; an inclusion such as $[x] \subset [-L, L]$ is checked on the computed endpoints.

Throughout this section, $J = [c_L, c_R]$ is one of the parameter intervals and $E = [e_u \; e_s]$ is a fixed invertible 2×2 matrix, an approximate eigenbasis of $DP_c(p_c)$. The point p_c is the fixed point of P_c given by Lemma 4.1 below, which also provides a box $\mathcal{K}_J \ni p_c$ for all $c \in J$. The *local map*

$$f_c(u,v) = E^{-1}\big(P_c(p_c + E(u,v)^T) - p_c\big)$$

satisfies $f_c(0,0) = 0$ for every $c \in J$. Given a box $B \subset \mathbb{R}^2$ in local coordinates, we say that intervals $[a_{ij}]$, $[h^i_{jk}]$, $[\partial_c f^i]$ *enclose the derivatives of f on $B \times J$* if, for all $(u,v) \in B$ and $c \in J$,

$$\partial_j f_c^i(u,v) \in [a_{ij}], \qquad \partial_j\partial_k f_c^i(u,v) \in [h^i_{jk}], \qquad \partial_c\big(f_c^i(u,v)\big) \in [\partial_c f^i],$$

where $\partial_1 = \partial_u$ and $\partial_2 = \partial_v$. Differentiating the definition of f_c gives

$$\partial_c f_c(u,v) = E^{-1}\big(\partial_c P_c(q) + (DP_c(q) - I)\, p_c'\big), \qquad q = p_c + E(u,v)^T. \tag{2}$$

Where the enclosures are computed. The fixed point p_c is only known to lie in the box $\mathcal{K}_J$. All enclosures are therefore computed on the interval hull of $(\mathcal{K}_J + E \cdot B) \times J$, and *not* around an approximate fixed point: we enclose DP_c, D^2P_c and $\partial_c P_c$ on this set, and $p_c' = dp_c/dc$ on $\mathcal{K}_J \times J$. Since this set contains $\{(p_c + E(u,v)^T, c) : (u,v) \in B,\ c \in J\}$, the resulting intervals enclose the derivatives of f on $B \times J$. The matrix E^{-1} is replaced by a rigorous interval enclosure computed by the adjugate formula.

4.2. **The fixed point.**

Lemma 4.1 (Krawczyk [22])**.** *Let $Q_{\mathcal{K}} \subset \mathbb{R}^2$ be a box, $\tilde{q} \in Q_{\mathcal{K}}$, and R a 2×2 matrix. Suppose that, for an interval $[c]$,*

$$\mathcal{K} = \tilde{q} - R\big([P_{[c]}(\tilde{q})] - \tilde{q}\big) + \big(I - R([DP_{[c]}(Q_{\mathcal{K}})] - I)\big)(Q_{\mathcal{K}} - \tilde{q})$$

is contained in the interior of $Q_{\mathcal{K}}$, where $[P_{[c]}(\tilde{q})]$ and $[DP_{[c]}(Q_{\mathcal{K}})]$ enclose $P_c(\tilde{q})$ and $DP_c(Q_{\mathcal{K}})$ for $c \in [c]$. Then for each $c \in [c]$ the map P_c has a unique fixed point p_c in $Q_{\mathcal{K}}$, and $p_c \in \mathcal{K}$.

(The inclusion $\mathcal{K} \subset \operatorname{int} Q_{\mathcal{K}}$ itself implies that R and all matrices in $[DP_{[c]}(Q_{\mathcal{K}})] - I$ are invertible; see [27, Chapter 5]. The programs take for R an approximate inverse of the midpoint of $[DP_{[c]}(Q_{\mathcal{K}})] - I$.)

Given $p_c \in \mathcal{K}_J$ for all $c \in J$, an enclosure of $p_c' = -(DP_c(p_c) - I)^{-1}\partial_c P_c(p_c)$ is obtained by evaluating this formula in interval arithmetic on $\mathcal{K}_J \times J$, the 2×2 inverse being computed by the adjugate formula after checking that the interval determinant does not contain 0.

4.3. **The local unstable manifold.**

Lemma 4.2. *Let $\delta, \rho, L, K, M > 0$ and $B_u = [-\delta,\delta]\times[-\rho,\rho]$. Let $[a_{ij}]$, $[h^i_{jk}]$, $[\partial_c f^i]$ enclose the derivatives of f on $B_u \times J$. Set*

$$\begin{aligned}
\Phi_1 &= [a_{11}] + [a_{12}][-L,L], \qquad \Psi_1 = [a_{21}] + [a_{22}][-L,L],\\
\Phi_2 &= [h^1_{11}] + 2[h^1_{12}][-L,L] + [h^1_{22}][0,L^2] + [a_{12}][-K,K],\\
\Psi_2 &= [h^2_{11}] + 2[h^2_{12}][-L,L] + [h^2_{22}][0,L^2] + [a_{22}][-K,K].
\end{aligned}$$

Assume:

(U1) $\operatorname{mig}\Phi_1 > 1$;
(U2) $L\delta \le \rho$;
(U3) $\Psi_1/\Phi_1 \subset [-L,L]$;
(U4) $(\Psi_2\Phi_1 - \Psi_1\Phi_2)/\Phi_1^3 \subset [-K,K]$;
(U5) $[\partial_c f^2] + [a_{22}][-M,M] - (\Psi_1/\Phi_1)\big([\partial_c f^1] + [a_{12}][-M,M]\big) \subset [-M,M]$;
(U6) *with* $m = \operatorname{mig}[a_{11}]$ *we have* $1 - \operatorname{mag}[a_{12}]L/m > 0$ *and* $\theta := \operatorname{mag}[a_{21}]\,\kappa + \operatorname{mag}[a_{22}](L\kappa+1) < 1$, *where* $\kappa = \dfrac{\operatorname{mag}[a_{12}]/m}{1-\operatorname{mag}[a_{12}]L/m}$.

Then for every $c \in J$ there is a function $w_c\colon [-\delta,\delta] \to [-\rho,\rho]$, real analytic in (u,c), such that:

(a) $w_c(0) = 0$, $|w_c'| \le L$, $|w_c''| \le K$ *and* $|\partial_c w_c| \le M$;
(b) $p_c + E(u, w_c(u))^T \in W^u(p_c)$ *for* $|u| \le \delta$;
(c) *if* $[a^0_{ij}]$ *enclose* $\partial_j f^i_c(0,0)$ *for* $c \in J$ *and* $t_0 \ge \operatorname{mag}\big([a^0_{21}]/([a^0_{11}] + [a^0_{12}][-L,L] - [a^0_{22}])\big)$, *then* $|w_c'(0)| \le t_0$, *and consequently* $|w_c(s)| \le t_0|s| + \frac{1}{2}Ks^2$ *and* $|w_c'(s)| \le t_0 + K|s|$.

The programs also check explicitly that $0 \notin [a_{11}]$ (which follows from (U1) anyway), so that m is the minimum of the moduli of the endpoints, and that the new graph stays in $|v| \le \rho$ (which follows from (U2)–(U3)).

Proof. The class. Let $\mathcal{G}_u$ be the set of functions $w\colon [-\delta,\delta]\times J \to \mathbb{R}$ such that, for each c, $w(\cdot,c)$ is C^1 with $w(0,c) = 0$, $|\partial_u w| \le L$ and $\partial_u w(\cdot,c)$ K-Lipschitz, and such that $c \mapsto w(u,c)$ is M-Lipschitz. By (U2), $|w| \le L\delta \le \rho$. By the Arzelà–Ascoli theorem, $\mathcal{G}_u$ is closed in C^0 with the sup norm.

Graph transform. For $w \in \mathcal{G}_u$ put $\phi(u,c) = f^1_c(u, w(u,c))$ and $\psi(u,c) = f^2_c(u,w(u,c))$; the points $(u, w(u,c))$ lie in B_u. Since $\partial_u\phi \in \Phi_1$, condition (U1) makes $\phi(\cdot,c)$ monotone with

$|\partial_u\phi| > 1$ and $\phi(0,c) = 0$, so $\phi([-\delta,\delta],c) \supset [-\delta,\delta]$. Define $(Tw)(\cdot,c) = \psi(\cdot,c) \circ \phi(\cdot,c)^{-1}$ on $[-\delta,\delta]$; its graph is the image of the graph of w, restricted to $|u| \le \delta$. If w is C^2, then

$$(Tw)' \circ \phi = \frac{\partial_u\psi}{\partial_u\phi}, \qquad (Tw)'' \circ \phi = \frac{\partial_u^2\psi\,\partial_u\phi - \partial_u\psi\,\partial_u^2\phi}{(\partial_u\phi)^3}, \qquad \partial_c(Tw)\circ\phi = \partial_c\psi - (Tw)'\circ\phi\cdot\partial_c\phi,$$

with $\partial_u\psi \in \Psi_1$, $\partial_u^2\phi \in \Phi_2$, $\partial_u^2\psi \in \Psi_2$, $\partial_c\phi \in [\partial_c f^1] + [a_{12}][-M,M]$ and $\partial_c\psi \in [\partial_c f^2] + [a_{22}][-M,M]$. By (U3)–(U5), T maps the analytic elements of $\mathcal{G}_u$ to analytic elements of $\mathcal{G}_u$.

Contraction. Let $w_1, w_2 \in \mathcal{G}_u$ and $x = \phi_1(u_1) = \phi_2(u_2)$. The mean value theorem applied to f^1 along the segment between $(u_1, w_1(u_1))$ and $(u_2, w_2(u_2))$ gives $m|u_1 - u_2| \le \operatorname{mag}[a_{12}](L|u_1 - u_2| + \|w_1 - w_2\|)$, so $|u_1 - u_2| \le \kappa\|w_1 - w_2\|$. Applied to f^2 it gives

$$|Tw_1(x) - Tw_2(x)| \le \operatorname{mag}[a_{21}]|u_1 - u_2| + \operatorname{mag}[a_{22}]\big(L|u_1 - u_2| + \|w_1 - w_2\|\big) \le \theta\|w_1 - w_2\|,$$

on all of $\mathcal{G}_u$, with $\theta < 1$ by (U6).

Fixed point. Starting from $w \equiv 0$, the iterates $T^n w$ are analytic elements of $\mathcal{G}_u$ forming a Cauchy sequence; their limit w_* lies in $\mathcal{G}_u$ and satisfies $Tw_* = w_*$. For u in the domain, $f_c(\phi^{-1}(u), w_*(\phi^{-1}(u))) = (u, w_*(u))$ with $|\phi^{-1}(u)| \le |u|/\operatorname{mig}\Phi_1$, so the backward orbit of every point of the graph stays on the graph and converges to 0. Hence the graph lies in $W^u(0; f_c)$, which proves (b).

Regularity. Let $\gamma(t,c)$ be an analytic parametrisation of a local unstable manifold $W^u_\eta(0; f_c)$ depending analytically on c (see e.g. [9]). Near $u = 0$ the graph coincides with $W^u_\eta(0; f_c)$, both being graphs over u of points whose backward orbits stay close to 0. For n large, the graph equals $f_c^n(\{(u, w_*(u)) : |u| \le \eta'\}) \cap \{|u| \le \delta\}$, so $w_*(u,c) = \pi_2 f_c^n(\gamma(t,c))$ where $t = t(u,c)$ solves $\pi_1 f_c^n(\gamma(t,c)) = u$. Since π_1 is strictly monotone along the graph by (U1), the analytic implicit function theorem shows that w_* is analytic in (u,c), and its Lipschitz bounds become the derivative bounds in (a). The saddle p_c, its local unstable manifold and the parametrisation γ continue analytically to c in an open interval containing J, and the non-degeneracy $\partial_t\pi_1 f_c^n(\gamma(t,c)) \ne 0$ is an open condition that holds on the compact set where it is used; so the same formula defines an analytic extension of w_* to a neighbourhood of $[-\delta,\delta] \times J$.

Part (c). The graph is tangent at 0 to the unstable eigenvector $(1,t)$ of $A = Df_c(0,0)$, so $t = w_c'(0)$ satisfies $t(a_{11} + a_{12}t - a_{22}) = a_{21}$ with $|t| \le L$, which gives the bound. The two consequences follow by integrating $|w_c''| \le K$. □

4.4. **The local stable manifold.**

Lemma 4.3. *Let $r_u, r_s, L_s, K_s, M_s > 0$ and $B_s = [-r_u, r_u] \times [-r_s, r_s]$. Let $[a_{ij}]$, $[h^i_{jk}]$, $[\partial_c f^i]$ enclose the derivatives of f on $B_s \times J$. Put*

$$\mathcal{D} = [a_{11}] - [-L_s, L_s][a_{21}], \qquad Z_1 = \frac{[-L_s, L_s][a_{22}] - [a_{12}]}{\mathcal{D}}, \qquad \zeta = \operatorname{mag} Z_1,$$

$$\Psi_s = [a_{21}][-\zeta,\zeta] + [a_{22}], \qquad Y_i = [h^i_{11}][0,\zeta^2] + 2[h^i_{12}][-\zeta,\zeta] + [h^i_{22}] \quad (i = 1,2).$$

Assume:

(S1) $\operatorname{mag}[a_{21}]\, r_u + \operatorname{mag}[a_{22}]\, r_s \le r_s$;
(S2) $\operatorname{mig}\mathcal{D} > 1$;
(S3) $m_s := \operatorname{mig}[a_{11}] - L_s \operatorname{mag}[a_{21}] > 0$ *and* $(\operatorname{mag}[a_{12}] + L_s \operatorname{mag}[a_{22}])\, r_s \le m_s\, r_u$;
(S4) $Z_1 \subset [-L_s, L_s]$;
(S5) $\big([-K_s, K_s]\Psi_s^2 + [-L_s, L_s]Y_2 - Y_1\big)/\mathcal{D} \subset [-K_s, K_s]$;
(S6) $\big([-L_s, L_s][\partial_c f^2] + [-M_s, M_s] - [\partial_c f^1]\big)/\mathcal{D} \subset [-M_s, M_s]$;
(S7) $\operatorname{mag}[a_{21}]\, L_s + \operatorname{mag}[a_{22}] < 1$.

Then for every $c \in J$ there is $\sigma_c\colon [-r_s, r_s] \to [-r_u, r_u]$, real analytic in (v, c), with $\sigma_c(0) = 0$, $|\sigma_c'| \le L_s$, $|\sigma_c''| \le K_s$ and $|\partial_c \sigma_c| \le M_s$, such that $\{(\sigma_c(v), v) : |v| \le r_s\} \subset W^s(0; f_c)$.

Proof. Let $\mathcal{G}_s$ be the analogous class of functions σ with $\sigma(0) = 0$ and the Lipschitz versions of the bounds. For $|v| \le r_s$, let $h(u) = f_c^1(u, v) - \sigma(f_c^2(u, v))$ for $|u| \le r_u$. By (S1), $|f_c^2(u, v)| \le r_s$, so h is defined; $h' = a_{11} - \sigma' a_{21}$, so $|h'| \ge m_s > 0$ by (S3); and $|h(0)| \le (\operatorname{mag}[a_{12}] + L_s \operatorname{mag}[a_{22}]) r_s \le m_s r_u$. So h has a unique zero u with $|u| \le r_u$; call it $(T_s\sigma)(v)$. Clearly $T_s\sigma(0) = 0$, and differentiating $f^1(T_s\sigma(v), v) = \sigma(f^2(T_s\sigma(v), v))$ gives

$$(T_s\sigma)' = \frac{\sigma' a_{22} - a_{12}}{a_{11} - \sigma' a_{21}}, \qquad \partial_c (T_s\sigma) = \frac{\sigma' \partial_c f^2 + \partial_c \sigma - \partial_c f^1}{a_{11} - \sigma' a_{21}},$$
$$(T_s\sigma)'' = \frac{\sigma''\,(F_2')^2 + \sigma'\, Y_2^* - Y_1^*}{a_{11} - \sigma' a_{21}},$$

where $F_2' = a_{21}(T_s\sigma)' + a_{22}$ and $Y_i^* = f_{uu}^i((T_s\sigma)')^2 + 2 f_{uv}^i (T_s\sigma)' + f_{vv}^i$, the derivatives of f being evaluated at $(T_s\sigma(v), v) \in B_s$. By (S4)–(S6), T_s maps the analytic elements of $\mathcal{G}_s$ into $\mathcal{G}_s$. For the contraction, with $u_i = T_s\sigma_i(v)$,

$$\operatorname{mig}[a_{11}]\,|u_1 - u_2| \le L_s \operatorname{mag}[a_{21}] |u_1 - u_2| + \|\sigma_1 - \sigma_2\|,$$

so $\|T_s\sigma_1 - T_s\sigma_2\| \le m_s^{-1} \|\sigma_1 - \sigma_2\|$, and $m_s \ge \operatorname{mig} \mathcal{D} > 1$ by (S2). Let σ_* be the fixed point, obtained as in Lemma 4.2. Then f_c maps $(\sigma_*(v), v)$ to $(\sigma_*(v_1), v_1)$ with $|v_1| \le (\operatorname{mag}[a_{21}] L_s + \operatorname{mag}[a_{22}])|v|$, so by (S7) forward orbits on the graph converge to 0. Analyticity, the analytic extension to a neighbourhood of $[-r_s, r_s] \times J$, and the derivative bounds follow as in Lemma 4.2, using the analytic local inverse of f_c. □

4.5. **The tangency function.** Let $N \ge 1$, let $S = [s_m - \Delta, s_m + \Delta] \subset (0, \delta]$, and let w_c, σ_c be given by Lemmas 4.2 and 4.3. For $s \in S$ and $c \in J$ define

$$X_0(s, c) = p_c + E\big(s, w_c(s)\big)^T, \qquad \Gamma(s, c) = P_c^N(X_0(s, c)), \qquad \begin{pmatrix} U \\ V \end{pmatrix} = E^{-1}\big(\Gamma(s, c) - p_c\big), \tag{3}$$

and, whenever $|V| \le r_s$, $g(s, c) = U - \sigma_c(V)$. By Lemma 4.2(b), $\Gamma(s, c) \in W^u(p_c)$, and $\partial_s \Gamma \ne 0$ because P_c^N is a local diffeomorphism. The function $\ell_c(q) = U(q) - \sigma_c(V(q))$ is defined and real analytic on the strip $\{p_c + E(u, v)^T : |v| < r_s\}$, with $\partial_u \ell_c = 1$, and its zero set there is the graph $\{(\sigma_c(v), v)\}$, an arc of $W^s(p_c)$ by Lemma 4.3. Thus g has exactly the form required in Definition 2.1; only the condition $|V| < r_s$ on $S \times J$ has to be checked. Since w_c and σ_c extend analytically (Lemmas 4.2 and 4.3), so does g, to a neighbourhood of $S \times J$.

Lemma 4.4 (chain rule)**.** *Write $D_N = DP_c^N(X_0)$, $H_N = D^2 P_c^N(X_0)$ and $\partial_c P^N = \partial_c P_c^N(X_0)$: derivatives of the N-th iterate of the Poincaré map, including the return-time corrections. Then*

$$\partial_s g = U_s - \sigma_c'(V) V_s, \qquad \partial_s^2 g = U_{ss} - \sigma_c''(V) V_s^2 - \sigma_c'(V) V_{ss},$$
$$\partial_c g = U_c - (\partial_c \sigma_c)(V) - \sigma_c'(V) V_c,$$

where

$$(U_s, V_s)^T = E^{-1} D_N\big(e_u + w_c'(s) e_s\big),$$
$$(U_{ss}, V_{ss})^T = E^{-1}\Big(H_N[e_u, e_u] + 2 w_c' H_N[e_u, e_s] + (w_c')^2 H_N[e_s, e_s] + w_c''(s)\, D_N e_s\Big),$$
$$(U_c, V_c)^T = E^{-1}\Big((D_N - I)\, p_c' + \partial_c w_c(s)\, D_N e_s + \partial_c P^N\Big).$$

Proof. This is the chain rule, using $\partial_s X_0 = e_u + w_c' e_s$, $\partial_s^2 X_0 = w_c'' e_s$ and $\partial_c X_0 = p_c' + (\partial_c w_c) e_s$; the term $-p_c'$ in (U_c, V_c) comes from the moving origin. □

4.6. **The tangency criterion.**

Lemma 4.5. *Let $S = [s_-, s_+]$, $J = [c_L, c_R]$, and let $g\colon S \times J \to \mathbb{R}$ be continuous, twice differentiable in s and differentiable in c. Assume:*
(T1) $\partial_s^2 g < 0$ *on* $S \times J$;
(T2) $\partial_s g(s_-, c) > 0 > \partial_s g(s_+, c)$ *for all* $c \in J$;
(T3) $g(s, c_L) < 0$ *for all* $s \in S$, *and* $g(s_0, c_R) > 0$ *for some* $s_0 \in S$;
(T4) $\partial_c g > 0$ *on* $S \times J$.
Then for each $c \in J$, $\partial_s g(\cdot, c)$ has a unique zero $s_*(c) \in (s_-, s_+)$, the maximiser of $g(\cdot, c)$; the function $G(c) = \max_S g(\cdot, c)$ is continuous and strictly increasing with a unique zero $c_* \in (c_L, c_R)$; at $(s_*(c_*), c_*)$ we have $g = \partial_s g = 0$, $\partial_s^2 g < 0$, $\partial_c g > 0$; and this is the only point of $S \times J$ where $g = \partial_s g = 0$. If g is C^2, then s_* and G are C^1 with $G'(c) = \partial_c g(s_*(c), c) > 0$.

Proof. By (T1) and (T2), $\partial_s g(\cdot, c)$ is strictly decreasing and changes sign on S, so it has a unique zero $s_*(c)$ in the interior, the maximiser of $g(\cdot, c)$. By compactness, G is continuous. By (T4) and the mean value theorem in c, $g(s, c_2) > g(s, c_1)$ for every s when $c_1 < c_2$, so G is strictly increasing; by (T3), $G(c_L) < 0 < G(c_R)$, and the intermediate value theorem gives the unique zero. If $g(s, c) = \partial_s g(s, c) = 0$, then $s = s_*(c)$ and $G(c) = 0$, so $c = c_*$. When g is C^2, the implicit function theorem shows that s_* is C^1 and $G' = \partial_c g + \partial_s g \cdot s_*' = \partial_c g(s_*(c), c)$. □

This lemma, except for its final optional regularity statement, has been formalised in Lean 4 (Section 7.2). The formal version assumes derivatives in the two-sided sense at every point of the closed rectangle $S \times J$; this holds for our g, which extends analytically to a neighbourhood of $S \times J$.

Remark 4.6 (how (T3) is checked). For $s \in S$, Taylor's formula and (T1) give

$$g(s, c_L) \le g(s_m, c_L) + \partial_s g(s_m, c_L)(s - s_m) - \tfrac{1}{2}\gamma(s - s_m)^2 \le g(s_m, c_L) + \frac{(\partial_s g(s_m, c_L))^2}{2\gamma},$$

where $\gamma = \min_S |\partial_s^2 g(\cdot, c_L)|$. It therefore suffices to enclose g and $\partial_s g$ at the single point (s_m, c_L), and $\partial_s^2 g$ on $S \times \{c_L\}$. This bound is also formalised in Lean.

5. The computer-assisted verification near $c = 5.7$

In this section we prove the following result, and deduce the Main Theorem.

Proposition 5.1 (computer-assisted)**.** *For $i = 1, 2, 3$ let $J_i = [c_L^{(i)}, c_R^{(i)}]$ be the intervals with the double-precision endpoints given in (4). Then*

$$J_1 \subset (5.6994199724,\, 5.6994199925), \qquad J_2 \subset (5.6995796078,\, 5.6995796081),$$
$$J_3 \subset (5.70005464309,\, 5.70005464312),$$

so that $|c - 5.7| < 5.81 \cdot 10^{-4}$, $< 4.21 \cdot 10^{-4}$ and $< 5.47 \cdot 10^{-5}$ on J_1, J_2, J_3 respectively. For each i:

(i) *For every $c \in J_i$ the map P_c has a unique fixed point p_c in the box $Q_{\mathcal{K},i}$, and p_c lies in the box Q_i (both boxes are given in Table 2). It is a dissipative flip saddle: $\lambda_u \in [-2.4040, -2.4037]$, $-1 < \lambda_s < 0$ and $|\lambda_u \lambda_s| < 2 \cdot 10^{-8}$.*
(ii) *There is $c_{*,i} \in J_i$ such that $W^u(p_{c_{*,i}})$ and $W^s(p_{c_{*,i}})$ have a quadratic homoclinic tangency which unfolds generically as c crosses $c_{*,i}$ (Definition 2.1). The tangency lies on the branch $P_c^{N_i}(W^u_{\mathrm{loc}}(p_c))$ of the unstable manifold, with $N_1 = 15$, $N_2 = 26$, $N_3 = 25$, within distance $4 \cdot 10^{-8}$ of $p_{c_{*,i}}$.*

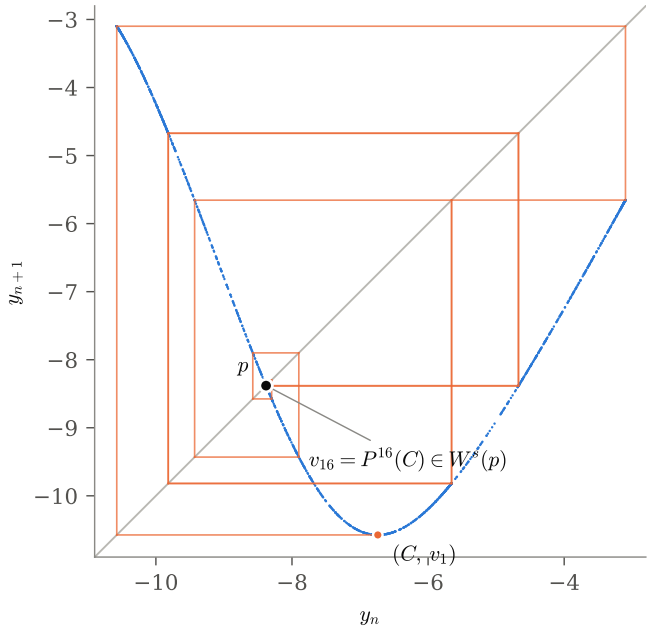


FIGURE 1. The return map at $c = c_0 \approx c_{*,3} \approx 5.70005$: pairs (y_n, y_{n+1}) along an orbit on the attractor (dots), and the cobweb of the critical orbit $C \mapsto v_1 \mapsto \cdots \mapsto v_{16}$. At $c_{*,3}$ the image v_{16} lands on the stable manifold of the saddle p: this is the homoclinic tangency of Proposition 5.1 for J_3, used in the Main Theorem. Non-rigorous double-precision computation.

5.1. **Numerical exploration (non-rigorous).** Near $c = 5.7$ the return map P_c contracts areas by a factor of about $3 \cdot 10^{-14}$ per iterate ($\lambda_u \approx -2.40$, $\lambda_s \approx -1.3 \cdot 10^{-14}$). Its attractor is therefore an extremely thin folded curve, and the dynamics is well described by the one-dimensional map $y_n \mapsto y_{n+1}$ (Figure 1), unimodal on the attractor with a minimum at a critical point C. The fixed point $p \approx (-8.381, 0.0296)$ lies on its decreasing branch.

A homoclinic tangency of p occurs when the fold of $W^u(p)$ at C is mapped onto $W^s(p)$; in the one-dimensional picture, when the critical point lands on p after n iterates. To locate such parameters we parametrise $W^u_{\mathrm{loc}}(p_c)$ by $s \mapsto p_c + se_u$; $K_2 = 9$ or 10 iterates bring this arc to the fold; we then compute the u-coordinate of $P_c^{K_2+n}(p_c + se_u)$ near its extremum in s, and find the zeros in c of the extremal value. Near 5.7 this gives tangency parameters for many values of n, on both sides of 5.7. We selected three of them, for $n = 6$ and $n = 16$, close to 5.7 (Table 2). The matrix E is the numerical eigenbasis of $DP_{c_0}(p_{c_0})$ at the numerical tangency parameter c_0. Figure 2 shows the unfolding for J_3. These approximate data only determine *where* the rigorous computation looks; they play no role in the logic of the proof.

5.2. **Implementation.** All computations in this section use the CAPD::DynSys library [20], version 6.1.0 (GitHub commit `2f06098`), compiled with `g++` 13.3. All the checks are implemented in one program, `tangency_cap.cpp`. The variants for the different intervals are generated from it by a script that substitutes only the numerical parameters and the numerical statement being checked; regenerating them reproduces the released files byte for byte.

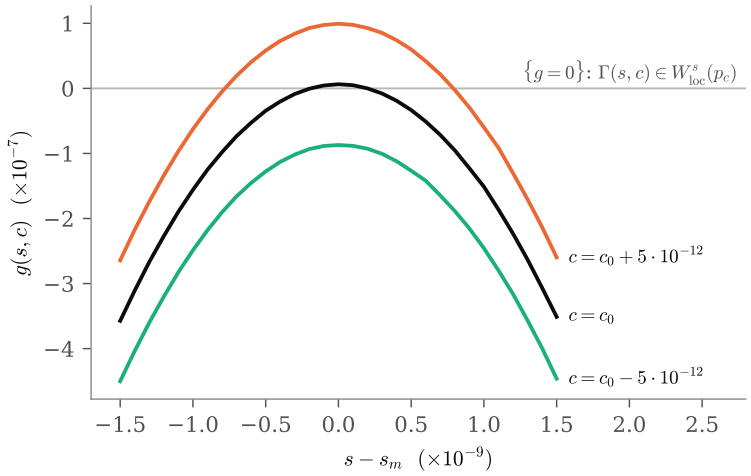


FIGURE 2. The tangency function $g(s,c)$ for J_3 near its maximum, for three parameter values around the numerical tangency parameter c_0. The maximum crosses 0 (the local stable manifold) with speed $\partial_c g \approx 1.86\cdot10^4$, and $\partial_s^2 g \approx -3.21\cdot10^{11}$. Non-rigorous double-precision computation; the rigorous enclosures are in Table 1.

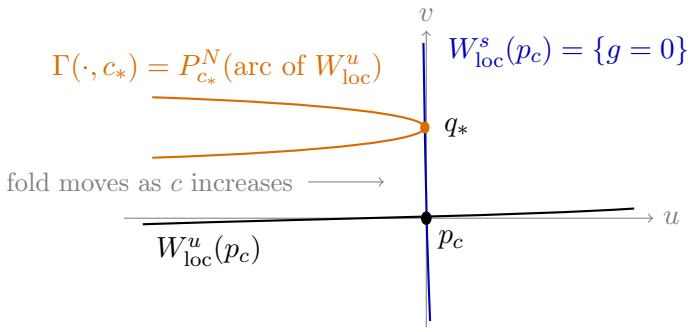


FIGURE 3. Schematic (not to scale) of the tangency in the local chart around p_c, with $N=25$ for J_3. The fold of the arc $\Gamma(\cdot,c)$ moves with speed $\partial_c g>0$ and touches the local stable manifold quadratically at $c=c_*$. In reality the fold is extremely thin, and the tangency point q_* lies within $4\cdot10^{-8}$ of p_{c_*}.

Integrator. Poincaré maps and their first and second derivatives are enclosed with the C^2-Lohner algorithm [23, 37], of Taylor order 20, applied to the extended four-dimensional field $\hat{X}$, with section $\{x=0\}$ crossed from $x<0$ to $x>0$.

Parameters. The parameters $a=b=0.2$ enter as the intervals $[2/10]$, which contain 0.2. For each i, $c^{(i)}_{\mathrm{mid}}$ is the double given in Table 2, and $J_i=[c^{(i)}_{\mathrm{mid}}-\varepsilon_c, c^{(i)}_{\mathrm{mid}}+\varepsilon_c]$ with endpoints

rounded to the nearest double; exactly,

$$
\begin{aligned}
J_1 &= [5.69941997244074549655579176032915711402893066406 25,\\
&\qquad 5.69941999244074537500637234188616275787353515625],\\
J_2 &= [5.69957960782199535287873004563152790069580078125,\\
&\qquad 5.69957960802199536942680424544960260391235351562 5],\\
J_3 &= [5.70005464309744258599721433711238205432891845703125,\\
&\qquad 5.70005464311744258765202175709418952465057373046875].
\end{aligned}
\tag{4}
$$

The programs check that $c_L, c_{\mathrm{mid}}, c_R \in J_i$.

Fixed point. The Krawczyk test of Lemma 4.1 is performed for $c \in J$ on the box $\tilde{q} + [\pm 3 \cdot 10^{-8}] \times [\pm 10^{-9}]$, and at the single values $c_L, c_{\mathrm{mid}}, c_R$ on boxes of radius 10^{-11} centred at $\tilde{q} + \tilde{p}'(c - c_{\mathrm{mid}})$, with $\tilde{p}'$ an approximation of p_c'. The images $\mathcal{K}_L, \mathcal{K}_{\mathrm{mid}}, \mathcal{K}_R$ of the thin tests are checked to lie in $\mathcal{K}_J$, so all four describe the same branch p_c.

Derivative boxes. As explained in Section 4.1, the derivatives used in Lemmas 4.2 and 4.3 are enclosed on the interval hulls of $\mathcal{K}_J + E \cdot B_u$ and $\mathcal{K}_J + E \cdot B_s$, with $c \in J$. The enclosures of $Df_c(0,0)$ used in Lemma 4.2(c) are taken on $\mathcal{K}_J \times J$, and on the thin enclosures $\mathcal{K}_L \times \{c_L\}$ and $\mathcal{K}_R \times \{c_R\}$.

Second derivatives. CAPD returns second-order Taylor coefficients, which we convert to second derivatives by doubling the diagonal entries (Section 7.3).

Initial sets. For the composite map P_c^N on $S \times J$, the initial set is an affine (Lohner doubleton) set $\hat{x} + A\, r_0 + r$ in the extended phase space, where $\hat{x} = (0, \tilde{p} + s_m e_u, c_{\mathrm{mid}})$ is a point, $\tilde{p}$ the midpoint of the thin Krawczyk enclosure $\mathcal{K}_{\mathrm{mid}}$ of $p_{c_{\mathrm{mid}}}$, the columns of A are e_u, e_s and $(\tilde{p}', 1)$, with $\tilde{p}'$ the midpoint of the enclosure $[p']$ of p_c', and $r_0 = (S - s_m,\ [w],\ J - c_{\mathrm{mid}})$ with $[w]$ a bound for $w_c(S)$ from Lemma 4.2(c). The box r absorbs rounding errors of $\hat{x}$ and the remainder $p_c - \tilde{p} - \tilde{p}'(c - c_{\mathrm{mid}}) \in (\mathcal{K}_{\mathrm{mid}} - \tilde{p}) + ([p'] - \tilde{p}')(J - c_{\mathrm{mid}})$. This set contains $\{X_0(s,c)\}$ for all $s \in S$ and $c \in J$ and keeps the strong correlation between the base point and the parameter; the derivative enclosures returned by CAPD are valid at every point of it. For the evaluations at the single parameters c_L and c_R used for (T3), the set is centred instead at the midpoint of $\mathcal{K}_L$ (respectively $\mathcal{K}_R$), with no parameter direction, and r contains $\mathcal{K}_L$ (respectively $\mathcal{K}_R$) minus that midpoint. We then evaluate the formulas of Lemma 4.4 in interval arithmetic, keeping $D_N e_u$ and $D_N e_s$ as single vectors to avoid spurious cancellation errors.

Proof parameters. They are listed in Table 2; in all cases $\rho = 10^{-5}$ and $r_u = r_s = 10^{-6}$. The bounds L, K, M, L_s, K_s, M_s are found by iterating the right-hand sides of (U3)–(U5) and (S4)–(S6) with a safety factor 1.05, and are then verified.

The statement itself. Besides the hypotheses of Lemmas 4.1–4.5, the programs check the numerical statement of Proposition 5.1 as printed: that the decimal box $Q_{\mathcal{K},i}$ lies in the Krawczyk box, that $\mathcal{K}_J \subset Q_i$, the range of λ_u (from $\lambda_u = \operatorname{tr} - \lambda_s$ and $|\lambda_s| \le |\det|/(\operatorname{mig} \operatorname{tr} -1)$), the bound on $|\det|$, and the bound on the distance of the tangency point to p (see the proof below). Decimal constants are converted to intervals exactly enclosing them.

5.3. **Results.** Each program performs 40 checks (35 for the hypotheses and 5 for the statement); all succeed for J_1, J_2 and J_3. Table 1 gives the main enclosures for J_3, the interval closest to 5.7, and Table 2 summarises all three.

Proof of Proposition 5.1. Fix $i \in \{1,2,3\}$. Lemma 4.1, applied as described above, gives the fixed point p_c, unique in the Krawczyk box, which contains $Q_{\mathcal{K},i}$, and lying in $\mathcal{K}_J \subset Q_i$. Let $\chi(\lambda) = \lambda^2 - \operatorname{tr} \cdot \lambda + \det$ be the characteristic polynomial of $Df_c(0)$. The trace and determinant enclosures give $\chi(1) > 0 > \chi(-1)$, hence $\lambda_u < -1 < \lambda_s < 1$; then $|\lambda_u \lambda_s| = |\det| < 2 \cdot 10^{-8}$,

Step	Quantity	Rigorous enclosure / bound
Lemma 4.1	p_c, $c \in J_3$	$[-8.38100671276265, -8.38100671273825]$ $\times[0.0295898183755, 0.0295898183762]$
	p_c'	$[-1.18898577, -1.18898576] \times [-0.0044333646, -0.0044333645]$
saddle	$\operatorname{tr} Df_c(0)$	$[-2.4039731272, -2.4039731256]$
	$\det Df_c(0)$	$[-1.97 \cdot 10^{-11},\ 1.98 \cdot 10^{-11}]$
Lemma 4.2	$\operatorname{mig} \Phi_1$	> 2.39
	$L,\ K,\ M$	$\le 9.74 \cdot 10^{-5},\ \le 3.74 \cdot 10^{-4},\ \le 6.35 \cdot 10^{-4}$
	θ	$\le 2.07 \cdot 10^{-4}$
	t_0 (on J_3; at c_L, c_R)	$\le 3.69 \cdot 10^{-12}$; $\le 3.83 \cdot 10^{-14}$
Lemma 4.3	$L_s,\ K_s,\ M_s$	$\le 2.85 \cdot 10^{-5},\ \le 0.714,\ \le 1.33 \cdot 10^{-4}$
	$(\operatorname{mig} \mathcal{D})^{-1}$	< 0.4160
(T3)	$g(s_m, c_L)$	$[-2.0093 \cdot 10^{-7}, -1.7142 \cdot 10^{-7}]$
	$\partial_s g(s_m, c_L)$	$[0.997,\ 1.834]$
	$\sup_S g(\cdot, c_L)$	$\le -1.7142 \cdot 10^{-7}$
	$g(s_m, c_R)$	$[1.7143 \cdot 10^{-7},\ 2.0070 \cdot 10^{-7}]$
(T2)	$\partial_s g(s_m - \Delta, c)$, $c \in J_3$	$[4.137,\ 5.107]$
	$\partial_s g(s_m + \Delta, c)$, $c \in J_3$	$[-2.281,\ -1.313]$
(T1)	$\partial_s^2 g$ on $S \times J_3$	$[-3.21014 \cdot 10^{11},\ -3.21010 \cdot 10^{11}]$
(T4)	$\partial_c g$ on $S \times J_3$	$[1.8564 \cdot 10^{4},\ 1.8657 \cdot 10^{4}]$
chart	$\lvert V\rvert$ on $S \times J_3$	$\le 2.43 \cdot 10^{-9}$ (required: $< r_s = 10^{-6}$)
	$\lvert U\rvert$ on $S \times J_3$	$\le 2.21 \cdot 10^{-7}$ (not required)
statement	λ_u; $\lvert q_* - p\rvert$	$[-2.403973128, -2.403973125]$; $\le 2.43 \cdot 10^{-9}$

TABLE 1. Rigorous enclosures for J_3 (the tangency closest to $c = 5.7$) produced by the CAPD program, rounded outwards. Here f_c is the local map in the coordinates (u, v) centred at p_c.

and $\lambda_u = \operatorname{tr} - \lambda_s$ with $|\lambda_s| \le |\det|/(\operatorname{mig} \operatorname{tr} - 1)$ gives the stated range of λ_u. By Section 2, $\det > 0$, so $\lambda_s < 0$. (The determinant enclosure of the CAPD program contains 0; it is the orientation argument that fixes the sign. The independent Kv enclosures of Section 7.1 are strictly positive.)

The hypotheses (U1)–(U6) and (S1)–(S7) are verified, so Lemmas 4.2 and 4.3 provide w_c and σ_c. The function g of (3) is defined on $S \times J_i$, since $|V| < r_s$ there. Lemma 4.4 and the CAPD enclosures yield (T1)–(T4) (for (T3) via Remark 4.6), and Lemma 4.5 gives $c_{*,i} \in (c_L, c_R)$ and s_* with $g = \partial_s g = 0$, $\partial_s^2 g < 0$ and $\partial_c g > 0$. By the discussion preceding Lemma 4.4, this is a quadratic homoclinic tangency unfolding generically, in the sense of Definition 2.1.

Finally, at the tangency $U = \sigma(V)$, so $|U| \le L_s|V|$, and the tangency point $q_* = p + Ue_u + Ve_s$ satisfies $|q_* - p| \le (L_s\|e_u\| + \|e_s\|) \sup_{S \times J} |V|$, which the programs bound by $3.13 \cdot 10^{-8} < 4 \cdot 10^{-8}$ (Figure 3). It differs from p, because $q_* = P^{N_i}(X_0)$ with $X_0 \ne p$ and P is injective. □

Remark 5.2 (uniqueness). Each $c_{*,i}$ is unique only for the tracked branch $\Gamma(S, c)$. In any generic unfolding of a dissipative homoclinic tangency, further tangencies of $W^u(p_c)$ and $W^s(p_c)$, created by longer iterates, accumulate at $c_{*,i}$ [28].

Remark 5.3 (sanity checks). The double-precision estimates of $\partial_s^2 g$ and $\partial_c g$ quoted in Figure 2 lie in the rigorous enclosures. As negative tests, we shifted each of $J_0, \dots, J_3$ by $\pm 3\varepsilon_c$, so that it no longer contains the tangency (the checks of the statement are then skipped): in all eight runs exactly one of the remaining 35 checks fails, namely (T3), at c_L for the positive shift and at c_R for the negative one, as predicted by $\partial_c g > 0$. The derivatives of P_c^N were also compared with finite differences (Section 7.3).

	J_1 $(n=6)$	J_2 $(n=16)$	J_3 $(n=16)$
c_{mid}	5.6994199824407454	5.6995796079219954	5.7000546431074426
ε_c, Δ	10^{-8}, 10^{-9}	10^{-10}, 10^{-10}	10^{-11}, 10^{-11}
K_2, N, δ	9, 15, $7\cdot10^{-4}$	10, 26, $6\cdot10^{-4}$	9, 25, $7\cdot10^{-4}$
s_m	$5.9787937263417563\cdot10^{-4}$	$2.486834987410949\cdot10^{-4}$	$5.9741814151543799\cdot10^{-4}$
$\tilde q$	$(-8.3802521043854075,$ $0.029592632330554456)$	$(-8.3804418993899592,$ $0.029591924532709056)$	$(-8.3810067127504517,$ $0.029589818375831582)$
$Q_{\mathcal K}$: y	$[-8.3802521343, -8.3802520744]$	$[-8.3804419293, -8.3804418694]$	$[-8.3810067427, -8.3810066828]$
$Q_{\mathcal K}$: z	$[0.029592631331, 0.029592633330]$	$[0.029591923533, 0.029591925532]$	$[0.029589817376, 0.029589819375]$
Q: y	$[-8.380252117, -8.380252092]$	$[-8.38044189952, -8.38044189926]$	$[-8.38100671277, -8.38100671273]$
Q: z	$[0.0295926320, 0.0295926327]$	$[0.0295919245296, 0.0295919245358]$	$[0.0295898183755, 0.0295898183762]$
$\operatorname{tr} Df_c(0)$	$[-2.40374631, -2.40374475]$	$[-2.403802784, -2.403802768]$	$[-2.4039731272, -2.4039731256]$
$\lvert\det Df_c(0)\rvert$	$<1.95\cdot10^{-8}$	$<1.96\cdot10^{-10}$	$<1.98\cdot10^{-11}$
$g(s_m, c_L)$	$[-9.2878, -9.2758]\cdot10^{-8}$	$[-2.8412, -2.8072]\cdot10^{-6}$	$[-2.0093, -1.7142]\cdot10^{-7}$
$g(s_m, c_R)$	$[9.2758, 9.2878]\cdot10^{-8}$	$[2.8069, 2.8412]\cdot10^{-6}$	$[1.7143, 2.0070]\cdot10^{-7}$
$\partial_s^2 g$	$[-1.60020, -1.59973]\cdot10^{8}$	$[-2.81306, -2.81237]\cdot10^{12}$	$[-3.21014, -3.21010]\cdot10^{11}$
$\partial_c g$	$[4.786, 13.78]$	$[2.380, 3.269]\cdot10^{4}$	$[1.8564, 1.8657]\cdot10^{4}$
$\lvert V\rvert$	$\le 2.02\cdot10^{-9}$	$\le 3.13\cdot10^{-8}$	$\le 2.43\cdot10^{-9}$

TABLE 2. The three tangencies near $c=5.7$ (CAPD). $\tilde q$ is the (exact double) centre of the Krawczyk box; $Q_{\mathcal K}$ is a decimal box inside the Krawczyk box (uniqueness of p_c), and Q a decimal box containing the Krawczyk image $\mathcal K_J$ (location of p_c). Enclosures are rounded outwards; those of $\partial_s^2 g$, $\partial_c g$ and $|V|$ are over $S\times J$. For J_1 and J_3 the eigenvector e_u is replaced by $-e_u$, so that $s>0$ reaches the fold after an odd number K_2 of iterates.

Proof of the Main Theorem. Let $c_* = c_{*,3}$ be the parameter given by Proposition 5.1 for $i=3$. Then $|c_*-5.7|<5.47\cdot10^{-5}$, the saddle p_{c_*} satisfies $|\det DP_{c_*}(p_{c_*})|<2\cdot10^{-8}<1$, and its stable and unstable manifolds have a quadratic homoclinic tangency unfolding generically at c_*. The first statement therefore follows from Proposition 3.5, and the second by taking $\varepsilon = 5\cdot10^{-6}$, since $(c_*-5\cdot10^{-6}, c_*+5\cdot10^{-6})\subset(5.7-6\cdot10^{-5}, 5.7+6\cdot10^{-5})$. The same argument applies to $c_{*,1}$, $c_{*,2}$ and to the band-merging parameter of Proposition 6.1. □

6. The band-merging tangency

Proposition 6.1 (computer-assisted)**.** *Let $J_0=[c_L^{(0)}, c_R^{(0)}]$, with the double-precision endpoints given in (5), so that $J_0\subset(4.506989336, 4.506989357)$. Then the conclusions (i)–(ii) of Proposition 5.1 hold on J_0, with the boxes $Q_{\mathcal K,0}$ and Q_0 given below, $\lambda_u\in[-1.92148,-1.92146]$, $|\lambda_u\lambda_s|<5\cdot10^{-8}$, $N_0=15$, and the tangency point within $2\cdot10^{-8}$ of $p_{c_{*,0}}$. Consequently, the conclusion of Proposition 3.5 holds near $c_{*,0}$.*

The same program, with the parameters of Table 3, proves Proposition 6.1. Here $K_2=12$ and $N=15$: the fold of $W^u(p)$ is mapped onto $W^s(p)$ after 3 further iterates. Numerically, this is the parameter at which the two bands of the chaotic attractor of the period-doubling cascade merge. The interval is

$$\begin{aligned} J_0 = [&4.5069893363119701845675990625750273466110229492187 5,\\ &4.5069893563119700630181796441320329904556274414062 5], \end{aligned} \tag{5}$$

the doubles nearest to $c_{\mathrm{mid}}\mp10^{-8}$, with c_{mid} the double nearest to 4.50698934631197. The Krawczyk test gives a unique fixed point in

$$Q_{\mathcal K,0} = [-6.9386987611,\ -6.9386987012]\times[0.0360634877,\ 0.0360634896],$$

Step	Quantity	Rigorous enclosure / bound
parameters	s_m, Δ, δ	$5.3682155586 \cdot 10^{-4}$, 10^{-9}, $6 \cdot 10^{-4}$
	E	$\begin{pmatrix} 0.9999996961880596 & -0.8077389541129416 \\ 7.795022697815469 \cdot 10^{-4} & -0.5895403141503822 \end{pmatrix}$
saddle	$\operatorname{tr} Df_c(0)$, $\det Df_c(0)$	$[-1.92147167, -1.92147014]$, $[-4.52, 4.53] \cdot 10^{-8}$
(T3)	$g(s_m, c_L)$, $g(s_m, c_R)$	$[-1.7531, -1.6882] \cdot 10^{-8}$, $[1.6881, 1.7529] \cdot 10^{-8}$
(T2)	$\partial_s g(s_m \mp \Delta, c)$	$[0.01908, 0.02497]$, $[-0.02557, -0.01967]$
(T1)	$\partial_s^2 g$ on $S \times J_0$	$[-2.23388, -2.23090] \cdot 10^7$
(T4)	$\partial_c g$ on $S \times J_0$	$[1.4164, 2.0247]$
chart	$\lvert V \rvert$ on $S \times J_0$	$\le 9.92 \cdot 10^{-9}$

TABLE 3. The band-merging tangency of Proposition 6.1 (CAPD), rounded outwards.

lying in $Q_0 = [-6.9386987439, -6.9386987185] \times [0.0360634882, 0.0360634892]$. All 40 checks succeed, and the shifted intervals $J_0 \pm 3 \cdot 10^{-8}$ fail at (T3) only, as expected. The proof of Proposition 6.1 is then identical to that of Proposition 5.1; here the distance of the tangency point to p is bounded by $9.92 \cdot 10^{-9} < 2 \cdot 10^{-8}$.

7. Independent verification, formal proof and code

7.1. **A second implementation with the Kv library.** We re-verified all hypotheses used in the proofs for J_1, J_3 and J_0 (the Krawczyk test, (U1)–(U6), (S1)–(S7), (T1)–(T4) and the chart condition), together with the numerical statements (exact endpoints of J, the boxes $Q_{\mathcal{K}}$ and Q, the range of λ_u and the bound on $|\det|$), with a separately written program built on Kv [21], a C++ library for verified numerical computation by M. Kashiwagi (version 0.4.62), instead of CAPD. Three features make this implementation differ in substance, not only in code.

- *Poincaré map as a fixed-time map.* Write $x = r\cos\theta$, $y = r\sin\theta$, and use $t = \theta + \pi/2$ as independent variable. Then
$$\frac{dr}{dt} = \frac{r(arS^2 - Cz)}{D}, \qquad \frac{dz}{dt} = \frac{r(b + z(rC - c))}{D},$$
where $C = \sin t$, $S = -\cos t$ and $D = r(1+aCS)+Sz = r\dot\theta$. The section Σ is $\{t \equiv 0 \bmod 2\pi\}$, so as long as $\dot\theta > 0$, P_c is exactly the time-2π map in the coordinates $(y, z) = (-r, z)$, and P_c^N the time-$2\pi N$ map: no return-time correction is needed. The condition $D > 0$ is enforced rigorously, since Kv's series division fails if the range of D contains 0 on any Taylor step. (A non-rigorous exploration, not used in the proof, gives $\dot\theta \ge 0.88$ on the relevant orbits.)
- *Jets.* First and second derivatives are obtained by integrating the first and second variational equations, written with forward-mode jet arithmetic inside the vector field, seeded along the directions actually needed (for example $e_u + w'e_s$ with w' an interval). In the c-slot, $D_N\tilde p' + \partial_c P^N$ is computed as a single directional derivative.
- *Sets.* All sets are Kv affine forms, propagated with the mean-value form of Kv's affine ODE solver, with noise symbols for s, c, the w-range and the remainder of p_c.

The one-step enclosures are Kv's own; the program adds a step-size strategy and exact power-of-two rescalings of the jet components, which do not affect rigour. It uses the same proof parameters as the CAPD programs, and its variants for J_1 and J_3 are generated from the program for J_0 by substituting only the numerical parameters and the numerical statement.

All 37 checks (32 for the hypotheses and 5 for the statement) succeed in each case, with runtimes on one core of 9, 13 and 7 minutes for J_1, J_3 and J_0. The Kv determinant enclosures

	Quantity	CAPD	Kv
J_3	$\det Df_c(0)$	$[-1.97, 1.98] \cdot 10^{-11}$	$[3.08113, 3.08114] \cdot 10^{-14}$
	$g(s_m, c_L)$	$[-2.0093, -1.7142] \cdot 10^{-7}$	$[-2.0885, -1.6210] \cdot 10^{-7}$
	$g(s_m, c_R)$	$[1.7143, 2.0070] \cdot 10^{-7}$	$[1.8007, 1.9247] \cdot 10^{-7}$
	$\partial_s^2 g$ on $S \times J_3$	$[-3.21014, -3.21010] \cdot 10^{11}$	$[-3.21015, -3.21009] \cdot 10^{11}$
	$\partial_c g$ on $S \times J_3$	$[1.8564, 1.8657] \cdot 10^{4}$	$[1.861053, 1.861065] \cdot 10^{4}$
J_1	$\det Df_c(0)$	$[-1.95, 1.95] \cdot 10^{-8}$	$[3.0897, 3.0957] \cdot 10^{-14}$
	$g(s_m, c_L)$	$[-9.2878, -9.2758] \cdot 10^{-8}$	$[-9.28208, -9.28140] \cdot 10^{-8}$
	$\partial_s^2 g$ on $S \times J_1$	$[-1.60020, -1.59973] \cdot 10^{8}$	$[-1.599966, -1.599959] \cdot 10^{8}$
	$\partial_c g$ on $S \times J_1$	$[4.786, 13.78]$	$[9.28165, 9.28190]$
J_0	$\det Df_c(0)$	$[-4.52, 4.53] \cdot 10^{-8}$	$[3.43502, 3.43503] \cdot 10^{-11}$
	$g(s_m, c_L)$	$[-1.7531, -1.6882] \cdot 10^{-8}$	$[-1.72066, -1.72056] \cdot 10^{-8}$
	$\partial_s^2 g$ on $S \times J_0$	$[-2.23388, -2.23090] \cdot 10^{7}$	$[-2.2323946, -2.2323828] \cdot 10^{7}$
	$\partial_c g$ on $S \times J_0$	$[1.4164, 2.0247]$	$[1.720502, 1.720572]$

TABLE 4. Independent verification: enclosures from the CAPD and the Kv programs, both rounded outwards.

are strictly positive, confirming $\lambda_s \in (-1, 0)$ independently of Section 2, and the Kv enclosures of det and $\partial_c g$ are much tighter than CAPD's; the others are comparable (Table 4). The negative tests (J_0 and J_3 shifted by $\pm 3\varepsilon_c$) fail exactly at (T3).

The Kv program was written independently of the CAPD program at the level of numerical method, library and code; however, it was produced with the same AI assistance (see the statement at the end) and has not yet been audited by an independent human expert. Its value is to rule out errors specific to one library, one integration scheme, or one implementation of the formula layer.

7.2. **Formalisation of the tangency criterion in Lean.** Lemma 4.5 and the bound of Remark 4.6 have been formalised in Lean 4 (v4.35.0) with Mathlib [26, 24] (commit `aa35a48`). The proofs contain no `sorry` and no additional axioms: `#print axioms` reports only `propext`, `Classical.choice` and `Quot.sound`. The main statement, slightly abridged, reads:

```
theorem tangency_criterion
  (hg  : ∀ s ∈ Icc sL sR, ∀ c ∈ Icc cL cR, HasDerivAt (fun s => g s c) (gs s c) s)
  (hgs : ∀ s ∈ Icc sL sR, ∀ c ∈ Icc cL cR, HasDerivAt (fun s => gs s c) (gss s c) s)
  (hgc : ∀ s ∈ Icc sL sR, ∀ c ∈ Icc cL cR, HasDerivAt (fun c => g s c) (gc s c) c)
  (hcont : ContinuousOn (fun p : ℝ × ℝ => g p.1 p.2) (Icc sL sR ×ˢ Icc cL cR))
  (hs : sL < sR) (hc : cL < cR)
  (hA : ∀ s ∈ Icc sL sR, ∀ c ∈ Icc cL cR, gss s c < 0)
  (hB : ∀ c ∈ Icc cL cR, 0 < gs sL c ∧ gs sR c < 0)
  (hC : (∀ s ∈ Icc sL sR, g s cL < 0) ∧ ∃ s₀ ∈ Icc sL sR, 0 < g s₀ cR)
  (hD : ∀ s ∈ Icc sL sR, ∀ c ∈ Icc cL cR, 0 < gc s c) :
  ∃ cstar ∈ Ioo cL cR, ∃ sstar ∈ Ioo sL sR,
    g sstar cstar = 0 ∧ gs sstar cstar = 0 ∧ gss sstar cstar < 0 ∧ 0 < gc sstar cstar ∧
    (∀ c ∈ Icc cL cR, ∃! s, s ∈ Icc sL sR ∧ gs s c = 0) ∧ ...
```

The omitted conclusions state that c_* is the unique zero of G on $[c_L, c_R]$, and that (s_*, c_*) is the only point of the rectangle where $g = \partial_s g = 0$. The formal proof follows the monotonicity argument of Lemma 4.5: it uses the mean value theorem, compactness and the intermediate value theorem, but not the implicit function theorem.

What is formalised is the deduction from (T1)–(T4) to the tangency; the graph-transform lemmas, the chain rule, the theory of Poincaré maps and the interval computations are not. A formal verification of the numerical part would require a verified validated ODE solver with

second-order variational equations, comparable to Immler's verification of Tucker's computation in Isabelle/HOL [19]; this does not currently exist in Lean.

7.3. **Code audit and release.** The points of the implementation where an error would be most consequential were checked as follows.

- *Derivatives of the Poincaré map, not of the flow.* In the CAPD programs, P, DP and D^2P are computed by CAPD's Poincaré-map routines (`computeDP`), which return the derivatives of the Poincaré map itself, including the first- and second-order corrections for the varying return time. Since c is a state variable of $\hat{X}$, the same correction applies to ∂_c. For P^N we integrate up to the N-th crossing and apply the same routine, which yields $D(P^N)$ and $D^2(P^N)$. A separate (non-rigorous) test program compares all first and second derivatives in the directions e_u, e_s and c, including those with respect to c and the Taylor-coefficient convention, with central finite differences of P_c^N at the point $X_0 = \tilde{p} + s_m e_u$ used in the proof and at a second point $\tilde{p} + \frac{1}{2} s_m e_u$ off the fold. For J_0 ($N = 15$), at both points, all entries larger than 0.1 in absolute value agree to within $9 \cdot 10^{-4}$ relative, most of them to 10^{-5}–10^{-8}. For J_3 ($N = 25$), at X_0 the first derivatives in the directions e_u and c and all second derivatives except those in the direction (e_s, e_s) agree to within $6 \cdot 10^{-3}$, those of size at least 10^7 (up to $4.5 \cdot 10^{11}$) to within $8 \cdot 10^{-4}$; at the second point the second derivatives (of size up to $5 \cdot 10^{15}$) vary on scales below the smallest usable step, and finite differences are inconclusive there. Entries that are small at the fold (the first derivatives along the strongly contracted direction e_s, and the second derivatives in the direction (e_s, e_s)) cannot be resolved by double-precision finite differences. In the Kv programs no correction is needed, since P_c is a fixed-angle map (Section 7.1); the overlap of the two sets of enclosures (Table 4) is therefore a further cross-check of the return-time corrections, including the c-direction and the N-fold composition.
- E^{-1}. In both implementations, E^{-1} is enclosed rigorously by the adjugate formula in interval arithmetic, after checking that the interval determinant does not contain 0.
- *Decisions.* Every check is decided by an interval comparison: an inequality between an endpoint and a constant, or an inclusion of intervals. Quantities such as mig and mag are computed from endpoints exactly. Midpoints are used only to choose the Krawczyk preconditioner and the centres of affine sets, whose remainders are included in the sets, so they do not affect rigour.
- *Enclosure boxes.* Derivatives are enclosed on $\mathcal{K}_J + E \cdot B$, as in Section 4.1.

The complete code, with build scripts, the full output logs, the negative tests and a script that rebuilds and reruns everything, is archived at Zenodo [DOI to be added] and mirrored at [repository URL to be added].

7.4. **Trust base.** Propositions 5.1 and 6.1 rest on: the mathematical arguments of Section 4, of which Lemma 4.5 is machine-checked; the correctness of the CAPD library, the compiler and the floating-point rounding modes, with, for J_1, J_3 and J_0, a second and independent implementation on the Kv library; and standard analytic facts (analytic dependence of local invariant manifolds, the implicit function theorem). Proposition 3.5, and hence the Main Theorem, additionally rests on the cited theorems of Mora–Viana, Benedicks–Young and Benedicks–Viana and, for the linearisation hypothesis (MV3), on Romero and Gonchenko–Shilnikov–Turaev (Remark 3.2).

8. Discussion: the classical parameter

The Main Theorem shows that SRB measures do occur in the Rössler family, in the same measure-theoretic sense as for the Hénon family, arbitrarily close to tangencies at distance less than $5.5 \cdot 10^{-5}$ from the classical value. They say nothing about a *specific* parameter. The parameter sets produced by Mora–Viana and Benedicks–Carleson-type exclusion arguments are Cantor-like, and certifying that one given parameter belongs to such a set would require controlling the critical orbit for all times; this has been done in one dimension only for special (for example Misiurewicz-type) parameters.

At $c = 5.7$ two scenarios are compatible with the rigorous results available: a non-uniformly hyperbolic attractor with an SRB measure, or a periodic sink of very long period with a tiny basin, embedded in a quasi-attractor. Galias's periodic window at distance less than $2 \cdot 10^{-22}$ from the classical parameters (in the direction $a = b$) [14] shows how closely the two interleave; the extremely small widths of the windows he found are, however, strong numerical evidence against the second scenario at the classical parameters themselves. Our results, which produce SRB parameters at distance of order 10^{-5} in the direction of c, are consistent with this picture: by Newhouse's phenomenon, the unfoldings of our tangencies also produce periodic sinks for parameters accumulating at each $c_{*,i}$.

In non-rigorous simulations, the largest Lyapunov exponent at $c = 5.7$ is about 0.071, and the sum of the exponents about -5.32. For a compactly supported invariant probability μ, the identities $\int \dot{x}\, d\mu = \int \dot{y}\, d\mu = 0$ give $\int x\, d\mu = a \int z\, d\mu$, so the μ-average of the sum of the Lyapunov exponents is $\int \operatorname{div} X_c\, d\mu = a - c + a \int z\, d\mu$. This makes the strong dissipativity quantitative, but does not exclude sinks.

Remark 8.1 (observable measures). At $(a, b, c) = (0.2, 0.2, 5.7)$, the box $W = [-10.7, -2.7] \times [0.028, 0.034]$ satisfies $P(W) \subset \operatorname{int} W$ (this is [20, Theorem 2]; we re-verified it with CAPD, enclosing the decimal endpoints by exact rational interval arithmetic). By the general theorem of Catsigeras and Enrich [11, Theorem 1], every continuous map of a compact set of positive Lebesgue measure has *SRB-like* (observable) measures; hence $P|_W$ has such measures, supported on $\bigcap_n P^n(W)$. This weak notion does not distinguish between the two scenarios above.

Shilnikov homoclinic orbits. Ding and Zheng [13] derive sufficient conditions for a homoclinic orbit of Shilnikov type to a saddle-focus, using series expansions of the solutions on its stable and unstable manifolds, and apply them to the Rössler system at one parameter set. A Shilnikov loop yields horseshoes nearby (and homoclinic tangencies in its unfoldings), but by itself it does not give SRB measures: horseshoes have zero Lebesgue measure and support no physical measure. To reach SRB measures one needs, as here, a generically unfolding tangency of a dissipative saddle together with the Mora–Viana and Benedicks–Viana theory. A computer-assisted proof of a Shilnikov loop, as in [10], would be a natural source of further tangencies, whose genericity for the Rössler family would still have to be checked.

Open problems.

(1) *More tangencies.* The method applies, with only numerical changes, to further tangencies of p from longer iterates, or to tangencies of periodic saddles of higher period; each successful run gives a further positive-measure set of SRB parameters. Whether tangency parameters accumulate at $c = 5.7$ is not known, and could not be established by finitely many such runs.

(2) *A fixed parameter.* Proving the existence of an SRB measure at $c = 5.7$ seems to require a finitely checkable condition implying non-uniform hyperbolicity for a single strongly dissipative folding map, for instance a two-dimensional analogue of computable Collet–Eckmann criteria. No such criterion is currently known. Galias's results [14] suggest that the classical attractor is not periodic, which is consistent with, but does not imply, the existence of an SRB measure.

Appendix A. Reproducibility

All programs, build scripts and output logs are archived at Zenodo [DOI to be added]:

- `tangency_cap.cpp`: the CAPD program for Proposition 6.1;
- `tangency_57_n6.cpp` (J_1), `tangency_57_n16b.cpp` (J_2), `tangency_57_n16a.cpp` (J_3): the CAPD programs for Proposition 5.1 (and the Main Theorem), generated from `tangency_cap.cpp` by `make_variant.py`;
- `tangency_kv.cpp` (J_0), `tangency_kv_n6.cpp` (J_1), `tangency_kv_n16a.cpp` (J_3): the Kv programs, with their headers and build script;
- `test_fd.cpp`: the finite-difference comparison of Section 7.3;
- `trap2.cpp`: the trapping-region check of Remark 8.1;
- `Criterion.lean`: the Lean formalisation.

Build and run, for example, with

```
g++ -O2 tangency_57_n16a.cpp $(capd-config --cflags --libs) -o tangency_57_n16a
./tangency_57_n16a
```

Optional arguments set ε_c and Δ, and shift c_{mid} for the negative tests. Every check prints `true`, and the program ends with `ALL CHECKS PASSED: true`. The Lean file is checked with `lake env lean` inside a Mathlib checkout at the commit given above.

Use of AI. The author made extensive use of an AI system (Claude Opus 5.5 extra, Anthropic) in this work, including for the computations, the programs and the preparation of the manuscript. The computer-assisted results can be reproduced with the published code.

References

[1] V. Araújo, M. J. Pacifico, E. R. Pujals, and M. Viana, *Singular-hyperbolic attractors are chaotic*, Trans. Amer. Math. Soc. **361** (2009), 2431–2485.

[2] Z. Arai and K. Mischaikow, *Rigorous computations of homoclinic tangencies*, SIAM J. Appl. Dyn. Syst. **5** (2006), 280–292.

[3] P. G. Barrientos and J. D. Rojas, *Typical coexistence of infinitely many strange attractors*, preprint, arXiv:2102.08316.

[4] M. Benedicks, *Non uniformly hyperbolic dynamics: Hénon maps and related dynamical systems*, survey, arXiv:math/0304450.

[5] M. Benedicks and L. Carleson, *The dynamics of the Hénon map*, Ann. of Math. **133** (1991), 73–169.

[6] M. Benedicks and M. Viana, *Solution of the basin problem for Hénon-like attractors*, Invent. Math. **143** (2001), 375–434.

[7] M. Benedicks and L.-S. Young, *Sinai–Bowen–Ruelle measures for certain Hénon maps*, Invent. Math. **112** (1993), 541–576.

[8] P. Berger, *Strong regularity. Abundance of non-uniformly hyperbolic Hénon-like endomorphisms*, Astérisque **410** (2019), 53–177.

[9] X. Cabré, E. Fontich, and R. de la Llave, *The parameterization method for invariant manifolds I: manifolds associated to non-resonant subspaces*, Indiana Univ. Math. J. **52** (2003), 283–328.

[10] M. J. Capiński and A. Wasieczko-Zając, *Computer assisted proof of Shil'nikov homoclinics: with application to the Lorenz-84 model*, SIAM J. Appl. Dyn. Syst. **16** (2017), 1453–1473.

[11] E. Catsigeras and H. Enrich, *SRB-like measures for C^0 dynamics*, Bull. Pol. Acad. Sci. Math. **59** (2011), 151–164.

[12] B. Coomes, H. Koçak, and K. J. Palmer, *A computable criterion for the existence of homoclinic tangencies*, J. Dynam. Differential Equations (2026), doi:10.1007/s10884-026-10533-y.

[13] Y. Ding and L. Zheng, *Existence of homoclinic orbit of Shilnikov type and the application in Rössler system*, Math. Comput. Simulation **206** (2023), 770–779, doi:10.1016/j.matcom.2022.12.013.

[14] Z. Galias, *Is the classical Rössler attractor periodic? A validated numerical study*, Chaos **36** (2026), no. 5, 053121, doi:10.1063/5.0301581.

[15] A. Gierzkiewicz and P. Zgliczyński, *Periodic orbits in Rössler system*, preprint, arXiv:2101.10406 (2021).

[16] S. V. Gonchenko, A. S. Gonchenko, A. O. Kazakov, and A. D. Kozlov, *Elements of contemporary theory of dynamical chaos: a tutorial. Part I. Pseudohyperbolic attractors*, Int. J. Bifurcation Chaos **28** (2018), 1830036.

[17] S. V. Gonchenko, L. P. Shilnikov, and D. V. Turaev, *On dynamical properties of multidimensional diffeomorphisms from Newhouse regions: I*, Nonlinearity **21** (2008), 923–972.

[18] E. Igra, *One dimensional dynamics and the Rössler attractor*, preprint, arXiv:2312.13840 (2023).

[19] F. Immler, *A verified ODE solver and the Lorenz attractor*, J. Automat. Reason. **61** (2018), 73–111.

[20] T. Kapela, M. Mrozek, D. Wilczak, and P. Zgliczyński, *CAPD::DynSys: a flexible C++ toolbox for rigorous numerical analysis of dynamical systems*, Commun. Nonlinear Sci. Numer. Simul. **101** (2021), 105578.

[21] M. Kashiwagi, *kv — a C++ library for verified numerical computation*, http://verifiedby.me/kv/, version 0.4.62.

[22] R. Krawczyk, *Newton-Algorithmen zur Bestimmung von Nullstellen mit Fehlerschranken*, Computing **4** (1969), 187–201.

[23] R. J. Lohner, *Computation of guaranteed enclosures for the solutions of ordinary initial and boundary value problems*, in: Computational Ordinary Differential Equations (J. R. Cash and I. Gladwell, eds.), Clarendon Press, Oxford, 1992, 425–435.

[24] The mathlib Community, *The Lean mathematical library*, in: Proceedings of the 9th ACM SIGPLAN International Conference on Certified Programs and Proofs (CPP 2020), 367–381.

[25] L. Mora and M. Viana, *Abundance of strange attractors*, Acta Math. **171** (1993), 1–71.

[26] L. de Moura and S. Ullrich, *The Lean 4 theorem prover and programming language*, in: Automated Deduction – CADE 28, Lecture Notes in Comput. Sci. **12699**, Springer, 2021, 625–635.

[27] A. Neumaier, *Interval Methods for Systems of Equations*, Encyclopedia of Mathematics and its Applications 37, Cambridge University Press, 1990.

[28] J. Palis and F. Takens, *Hyperbolicity and Sensitive Chaotic Dynamics at Homoclinic Bifurcations*, Cambridge Studies in Advanced Mathematics 35, Cambridge University Press, 1993.

[29] N. Romero, *Persistence of homoclinic tangencies in higher dimensions*, Ergodic Theory Dynam. Systems **15** (1995), 735–757.

[30] O. E. Rössler, *An equation for continuous chaos*, Phys. Lett. A **57** (1976), 397–398.

[31] S. Sternberg, *On the structure of local homeomorphisms of euclidean n-space, II*, Amer. J. Math. **80** (1958), 623–631.

[32] W. Tucker, *A rigorous ODE solver and Smale's 14th problem*, Found. Comput. Math. **2** (2002), 53–117.

[33] M. Viana, *Dynamics: a probabilistic and geometric perspective*, in: Proceedings of the International Congress of Mathematicians, Vol. I (Berlin, 1998), Doc. Math. Extra Vol. ICM 1998, 557–578.

[34] D. Wilczak, S. Serrano, and R. Barrio, *A mechanism for growth of topological entropy and global changes of the shape of chaotic attractors*, Chaos **35** (2025), no. 10, doi:10.1063/5.0284636.

[35] D. Wilczak and P. Zgliczyński, *Computer assisted proof of the existence of homoclinic tangency for the Hénon map and for the forced damped pendulum*, SIAM J. Appl. Dyn. Syst. **8** (2009), 1632–1663.

[36] D. Wilczak and P. Zgliczyński, *Period doubling in the Rössler system—a computer assisted proof*, Found. Comput. Math. **9** (2009), 611–649.

[37] D. Wilczak and P. Zgliczyński, *C^r-Lohner algorithm*, Schedae Informaticae **20** (2011), 9–46.

[38] L.-S. Young, *What are SRB measures, and which dynamical systems have them?*, J. Stat. Phys. **108** (2002), 733–754.

[39] P. Zgliczyński, *Computer assisted proof of chaos in the Rössler equations and in the Hénon map*, Nonlinearity **10** (1997), 243–252.

Laboratoire d'Océanographie Physique et Spatiale, Univ Brest, CNRS, Ifremer, IRD, Brest, France

Email address: theophile.caby@univ-brest.fr